Generating low-voltage grid proxies in order to estimate grid capacity for residential end-use technologies: The case of residential solar PV

(article starts on next page)

Method Article

Generating low-voltage grid proxies in order to estimate grid capacity for residential end-use technologies: The case of residential solar PV

Elias Hartvigsson [a],[*], Mikael Odenberger [a], Peiyuan Chen [b], Emil Nyholm [a]

[a] Department of Space Earth and the Environment, Division of Energy Technology, Chalmers University of Technology Sweden
[b] Department of Electrical Engineering, Division of Electric Power Engineering, Chalmers University of Technology Sweden

A B S T R A C T

Due to data restrictions and power system complexity issues, it is difficult to estimate grid capacity for solar PV on regional or national scales. We here present a novel method for estimating low-voltage grid capacity for residential solar PV using publicly available data. High-resolution GIS data on demographics and dwelling dynamics is used to generate theoretical low-voltage grids. Simplified power system calculations are performed on the generated low-voltage grids to estimate residential solar PV capacity with a high temporal resolution. The method utilizes previous developments in reference network modelling and solar PV hosting capacity assessments. The method is demonstrated using datasets from Sweden, UK and Germany. Even though the method is designed to estimate residential solar PV grid capacity, the first block of the method can be utilized to estimate grid capacity or impacts from other residential end-use technologies, such as electric heating or electric vehicle charging.

This method presents:

- A method for estimating peak demand based on population density and dwelling type.
- Generation of low-voltage grids based on peak demand.
- Sizing of transformers and cables based on national low-voltage regulations and standards.

* Corresponding author.
E-mail address: Elias.hartvigsson@chalmers.se (E. Hartvigsson).

Specifications table

Subject area:	Engineering
More specific subject area:	*Electric power engineering*
Method name:	*Open LV-Grid Generator*
Name and reference of original method:	M. Hyvärinen, "Electrical networks and economies of load density," Helsinki University of Technology, 2008
Resource availability:	Data is published in [1] and hosted at the Mendeley Data repository http://dx.doi.org/10.17632/hn3ncrrj95.1 The computer code is available on Github http://dx.doi.org/10.5281/zenodo.4563951

Method details

Overview

To make traditional estimations of solar PV hosting capacity highly detailed data on grid components and layout is required. National data on grid components and topology are often distributed amongst tens to hundreds of operators. Furthermore, due to the infrastructure importance of electric power system, data often has security restrictions, further reducing accessibility to data. These data issues present a major barrier to estimating national levels of hosting capacity for solar PV. Yet, even with access to large datasets, the size and complexity of grids make traditional detailed power flow analysis unfeasible.

We solve these issues by generating theoretical low-voltage grids using national specific standards and demand estimation methods together with high-resolution geographical information system layers of demographics. The approach to assess hosting capacity of residential low voltage grids draws on previous research within Engineering Economic Approaches [2], reference network Modelling [3–5] and hosting capacity calculations [6]. Following most hosting capacity studies, we consider limits from capacity constraints of power system components and voltage variations at the Point of Common Connection (PCC). Voltage quality is determined based on voltage deviation and duration from its nominal value set by national and European regulations while capacity constraints are regulated by thermal limits from component standards. We are interested in estimating the technical hosting capacity, and therefore exclude economic limitations [7]. The presented method has been used to provide estimates of residential solar PV hosting capacity for Sweden, Germany and the UK [8].

Low-voltage grid hosting capacity is calculated in two modelling blocks consisting of four modelling steps. The first model block generates the low-voltage grids and includes the first three modelling steps (GIS load modelling, Transformer capacity allocation and Feeder length and feeder capacity estimation). The second model block focus on grid operation, including operational regulations, and the fourth modelling step, Hosting capacity calculation. Model block number one can be used to developed theoretical low-voltage grids that can be used to estimate grid capacity or grid impacts from other residential end-use technologies, while model block number two is specific for residential solar PV. Fig.1 shows a conceptual overview of the model. Hosting capacity is calculated in grid cells (1×1 km^2). We assume that each household has a connection to a national low-voltage grid. The customers grid connection is often regulated by national laws. In countries that allow for off-grid households, their total number is likely very small with negligible impact on the national residential solar PV hosting capacity.

GIS load model

To estimate the total peak demand in each grid cell we use country specific methods to estimate peak demand. The methods require information on the number of customers (*NC*), and their type, single family dwelling or apartment. Information on number of customers is obtained from high resolution GIS data on population density (1×1 km^2) and assuming average national household size. The distribution of dwelling type is generally not available with a high geographical resolution.
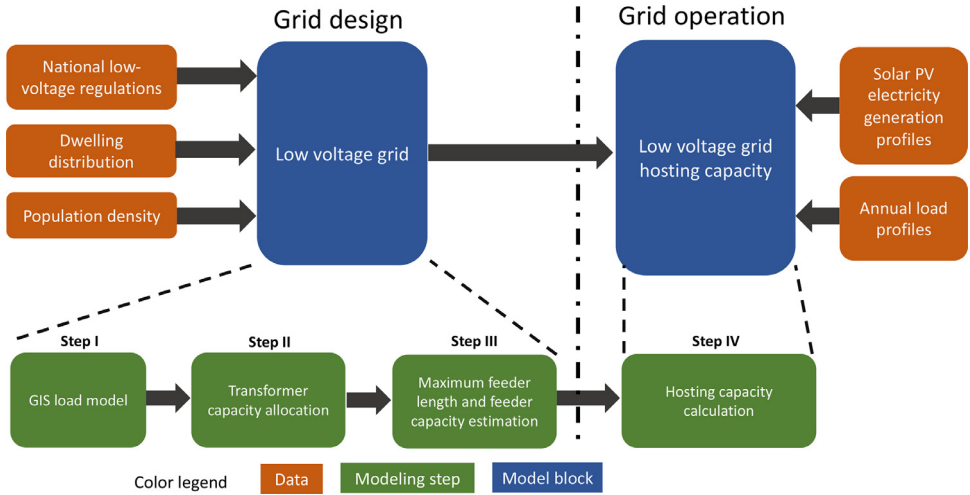
Fig. 1. Conceptual model framework, including the reference network model for the low-voltage grid and calculation of hosting capacity.
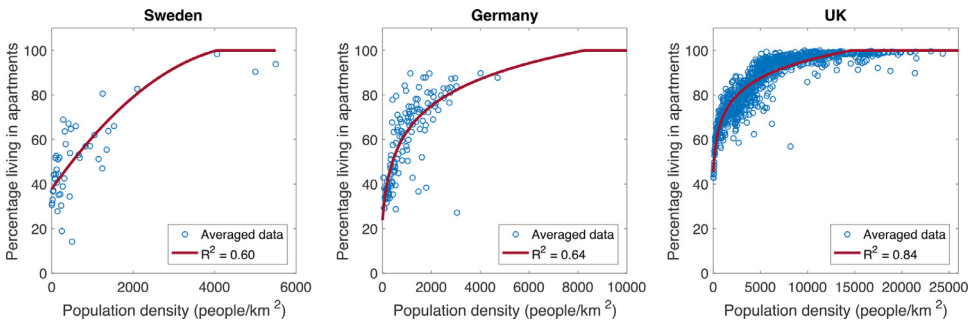

Fig. 2. Distribution of dwelling as a function of population density for Sweden Germany and UK. Circles shows averaged data on dwelling distribution taken from the 2011 European Census[9] for smallest available administrative regions and the corresponding population density. The red line shows the least square regression function.

Table 1

The corresponding datapoint where 100% of the population lives in apartments.

	Sweden	Germany	UK
Population density with 100% of population living in apartments (people/km^2)	4000	14690	8270

We use data on dwelling distribution on the highest available geospatial resolution (NUTS3 for the UK and Germany and LAU level for Sweden [9]) and population density [10] to map population density with the fraction of population living in apartments. The relationship between dwelling type and population density (f) is obtained by minimizing the error between data points and a set of functions (Fig. 2 and Eqs. (1)–(3)). The functions are assumed to be asymptotic and the convergence value is estimated based on the corresponding country's data and function f (Table 1). The functions considered are: polynomials up to order 8 and logarithmic functions of the type: $a \cdot \ln(b \cdot \rho + c)$, where a, b and c are constants. There is a significant variation in the area and population covered by NUTS3 and LAU areas. The variation lead to some large areas, where most of the population lives in cities, to have very low population density and a high share of population living in apartments (e.g.

Umeå municipality in Sweden where 77% of the population lives in areas with a population density larger than 1000/ people/km^2 but where the municipality's population density is 53 people/km^2). These types of areas likely eliminate some of the dwelling dynamics found in the grid cells. To remove the impacts of these outliers from the original NUTS3 and LAU dataset on the trend in dwelling dynamics, datapoints within a tenth of people/km^2 are averaged. This reduces the number of datapoints from 290 to 48 (Sweden), from 412 to 139 (Germany) and from 10310 to 1028 (UK). While this process reduce number of datapoints, it likely clarifies high-resolution dwelling dynamics.

Eqs. (1)–(3) shows the function mapped for each country's dwelling data, Eq. (1) (Sweden), Eq. (2) (Germany) and Eq. (3) (UK). The functions, and function parameters, were fitted to reduce the least square error.

$$f_{SWE}(\rho) = -2.5797 \cdot 10^{-8} \cdot \rho^2 + 0.000257 \cdot \rho + 0.3782 \tag{1}$$

$$f_{DE}(\rho) = 0.1812 \cdot \ln(0.0297 \cdot \rho + 3.6815) \tag{2}$$

$$f_{UK}(\rho) = 0.1173 \cdot \ln(0.34 \cdot \rho + 47.8547) \tag{3}$$

where ρ is the population density. Given a specific population density (ρ), the number of apartment customers (NC_{Apt}) and number of house customers (NC_{House}) can be calculated as follows.

$$NC_{Apt} = NC_{Total} \cdot f(\rho) \tag{4}$$

$$NC_{House} = NC_{Total} \cdot (1 - f(\rho)) \tag{5}$$

For each grid cell, peak power demand, $P_{D,Total}$, is estimated using country specific methods. We use Velander's formula for Sweden Eqs. (6) and (7), After Diversity Maximum Demand (ADMD) for the UK [11] Eqs. (8) and (9) and coincidence for Germany [12,13] Eqs. (10)–(12).

$$P_{D,Total,SWE}$$
$$= \left(E_{Total,SWE} \cdot \left(k_{1,apt} \cdot f(\rho) + k_{1,House} \cdot (1 - f(\rho)) \right) + \left(k_{2,apt} \cdot f(\rho) + k_{2,House} \cdot (1 - f(\rho)) \right) \cdot \sqrt{E_{Total,SWE}} \right) \tag{6}$$

$$E_{Tr,SWE} = \left(NC_{Total} \cdot f(\rho) \cdot E_{Apt} + NC_{Total} \cdot (1 - f(\rho)) \cdot E_{House} \right) \tag{7}$$

$$P_{D,Tr,UK} = NC_{Total} \cdot ADMD_{NCTotal} \cdot Ft \cdot \left(1 + \frac{12}{ADMD_{NCTotal} \cdot NC_{Total}} \right) \tag{8}$$

$$ADMD_{NCTotal} = ADMD_{Apt} \cdot f(\rho) + ADMD_{House} \cdot (1 - f(\rho)) \tag{9}$$

$$P_{D,Total,DE} = NC_{Tr} \cdot g_{NC_{Total}} \cdot P_{peak} \tag{10}$$

$$g_{NC_{Total}} = g_\infty + \frac{1 - g_\infty}{NC_{Total}^{3/4}} \tag{11}$$

$$P_{peak} = P_{Apt} \cdot f(\rho) + P_{House} \cdot (1 - f(\rho)) \tag{12}$$

where NC_{Total} is the number of customers per grid cell, $k_{1,apt}$, $k_{2,apt}$, $k_{1,House}$, and $k_{2,House}$ are the Velander coefficients, E_{Apt} and E_{House} annual per customer electricity consumption. The ADMD method used in the UK requires an $ADMD_{Apt}$ and $ADMD_{House}$ coefficient and a correction factor Ft. The German method requires coincidence for an infinite number of customers (g_∞) and power demand of apartments (P_{Apt}) and single-family dwellings (P_{House}) respectively. Tables 8–10 shows parameter values and sources for each country's power estimation method.
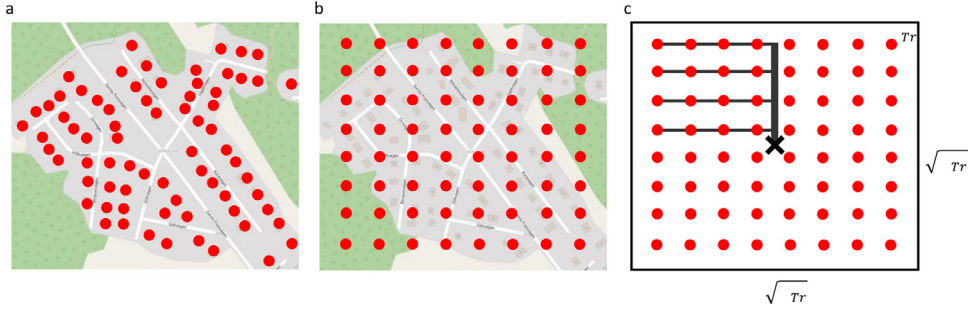
Fig. 3. Example of the uniform distribution of customers (red dots) and its impact compared to an actual distribution of customers. Actual customer distribution is taken from a suburban area outside Gothenburg, Sweden with an area A_{Tr} and length and width $\sqrt{A_{Tr}}$ using OpenStreetMap (© OpenStreetMap Contributors) (a), uniform distribution of customers (b) and uniform distribution, transformer placements, feeder and branches (c). The model assumes customers to be distributed uniformly within squares and therefore requires an equal number of customers horizontally and vertically. The number of customers in each Transformer Area (A_{Tr}) is therefore rounded to the closest integer of $\sqrt{A_{Tr}}$. Note that the actual distribution of customers is not generally accessible from OpenStreetMap.

Transformer capacity allocation

To estimate number (NT) and size (TR_{Cap}) of transformers we use a simple cost-minimization function of transformer and cable costs. In order to calculate cable costs, we use a low-voltage grid topology assuming uniformly distributed customers [2]. Fewer, but larger medium- to low-voltage transformers require longer low-voltage cables or power lines. More, but smaller transformers require longer medium-voltage cables or power lines. Furthermore, transformers are available in discrete sizes and are subject to economics of scale with decreasing cost per kVA for increasing transformer size. Since the number of customers per transformer is dependent on the number and capacity of the transformers, the GIS load model is evaluated iteratively with the transformer capacity allocation process. The cost, C_i, for each transformer size i in each grid cell, is calculated using Eqs. (13)–(17). The transformer size that results in the lowest cost in each grid cell is then set as the transformer size for that grid cell.

$$C_i = NT_i \cdot C_{Tr,i} + l_{LV,i} \cdot C_{LV} + l_{MV,i} \cdot C_{MV} \qquad i \in I \tag{13}$$

$$TR_{Cap,i} = \alpha \cdot P_{D,Tr} \qquad i \in I \tag{14}$$

$$l_{LV,i} = NC_{Tr,i} \cdot \sqrt{\frac{A_{NT,i}}{NC_{Tr,i} + 1}} \qquad i \in I \tag{15}$$

$$l_{MV,i} = NT_i \cdot \frac{1}{\sqrt{NT_i + 1}} \qquad i \in I \tag{16}$$

$$NC_{Tr,i} = \frac{NC_{Apt} + NC_{House}}{NT_i} \qquad i \in I \tag{17}$$

where I is the set of all possible transformer capacities (Table 7), $C_{Tr,i}$ is the cost per transformer with capacity i, NT_i the number of transformers with capacity i, C_{LV} and C_{MV} is the cost/km for low-voltage and medium voltage power lines respectively, and $l_{LV,i}$ and $l_{MV,i}$ total power line length for low and medium voltage respectively required for transformer capacity i. $l_{MV,i}$ is calculated assuming a uniform distribution of medium-low voltage transformers, in the same way as low-voltage customers, and therefore assumes a radial connection of transformers. See Fig. 3. To increase speed, cable costs in the cost minimization are therefore assumed for average sized power lines. $P_{D,Tr}$ is calculated iteratively using Eqs. (6)–(12) based on number of customers per transformer. To avoid replacing

Table 2

Data and sources for transformer costs and specifications. All sizes are considered in the cost-minimization for Sweden and Germany, but for the UK, 50 kVA transformers are excluded [14].

Transformer capacity (kVA)	50	100	200	315	500	800	1250
Cost (kSEK) [15]	32	38	54	71	102	135	195
Impedance (%)[1]	4	4	4	4	6	6	6
X/R ratio[2]	3	3	4	4	5	8	9
Earthing impedance (mΩ) [16]	130	65	32	20	13	10	6.5

1. Assumed
2. Assumed

Table 3

Low voltage (400V) line cost for different demographic areas. Costs taken for smallest available cable size in each area to reflect unequal working associated costs.

Area	City	Suburban	Rural
Distribution line cost (kSEK/km) [15]	827	540	177

Table 4

Medium voltage (12 kV, 240 mm^2) line cost for different demographic areas.

Area	City	Suburban	Rural
Distribution line cost (kSEK/km) [15]	1 004	691	358

transformers when demand increased, and to consider that transformer sizing is realistically not optimized, transformers are sized with an additional margin (α).

The cost of power lines per km is highly dependent on the type of demographic area, with considerably higher cost in dense suburban areas than sparse rural areas. The power line cost (C_{LV}) is therefore dependent on demographic area type [15,17]. Three commonly used demographic area types for low-voltage analysis are: city, suburban and rural. Demographic areas are generally not determined based on population density, and we therefore create a classification using area classifications from Statistics Sweden [18] and the Swedish Mapping, Cadastral and Land Registration Authority [19]. Our area classifications are defined accordingly: city/urban (population density$\geq$1000 people/km^2), suburban (1000 people/km^2 >population density$\geq$200 people/km^2), and rural (200 people/km^2 >population density). The dwelling type and prevalence of low-rise residential buildings is comparably similar in all countries, and the classification is therefore assumed to also be valid for Germany and the UK. We use power system components costs published by Swedish Energy Market Inspectorate [15] (Tables 3 and 4). Power system component costs are likely similar in Germany and the UK. Even if there are differences in costs, the cost-minimization function is dependent on relative cost difference between transformers and cables, which is likely more similar than absolute costs.

Distribution line costs used in the cost-minimization function for calculating allocation of transformers are taken from the Energy Market Inspectorate [15]. The costs are based on responses from Swedish DSOs about their purchase costs and is assumed to reflect real costs. Table 3 and 4 shows costs for distribution lines for different demographic areas. Due to differences in costs for groundwork, there is a significant cost difference between city and rural areas. Technical data for different distribution lines are shown in Table 5. Costs for common transformer sizes are also taken from the Swedish Energy Market Inspectorate [15], and are shown in Table 2. All sizes are considered in the cost-minimization for Sweden and Germany, but for the UK 50 kVA transformers are excluded [14].

The actual distribution of transformers and power lines is not limited to cost but includes additional factors such as reliability and ground topology (hills, lakes, rivers, buildings, and roads), and is dependent on the topology of the supplying medium voltage grid.

Table 5

Current rating for PVC insulated underground cables at 20 °C for sizes based on commonly used low-voltage distribution line sizes (<1000V) [15,22].

Cable type and size	Cu 10 mm^2	Cu 16 mm^2	Al 35 mm^2	Al 50 mm^2	Al 95 mm^2	Al 150 mm^2	Al 240 mm^2	Al 300 mm^2
Thermal capacity (A) [23]	52	67	80	94	138	178	230	345
Cable resistance [24] (Ω/km)	1.83	1.15	0.76	0.641	0.32	0.206	0.125	0.062[1]
Cable reactance (Ω/km)[2]	0.0861	0.0817	0.0783	0.0779	0.0762	0.0745	0.0752	0.0752[3]
Earthing impedance (Ω/km) [23]	4.18	2.63	1.91	1.47	0.746	0.495	0.324	0.299[4]

[1] Interpolated.
[2] Author elaborated based on [43].
[3] Assumed.
[4] Interpolated.

Maximum feeder length and capacity calculation

In order to calculate the feeder's length and number of branches we use an existing low-voltage topology [2]. The topology assumes that customers are uniformly distributed within each transformer area (see Fig. 3). The feeder and its branches are then sized based on national standards and regulations.

Based on the number of transformers (NT), each area is divided into NT number of smaller areas, each supplied by a single transformer. As the exact position of each customer is unknown, the customers are assumed to be distributed uniformly within each area, and the transformer placed in the centre (Fig. 3). We assume that transformer areas are squares with an area A_{Tr}, and that each customer must be reached with a horizontal or vertical feeder or branch originating from the transformer. To avoid over-branching and placing the PCCs to dense we limit the number of branches for each low-voltage feeder to five. Using basic geometrical relationships, the maximum feeder length can be calculated as

$$l_{max} = \sqrt{A_{Tr}} \frac{\left(\sqrt{NC_{Tr}} - 1\right)}{\sqrt{NC_{Tr}}} \cdot \gamma \tag{18}$$

where NC_{Tr} is the number of customers per transformer and A_{Tr} area each transformer supplies. Feeders are generally not drawn in straight lines, as such we use an adjustment factor γ [2]. If the number of customers per transformer is either 1 or 2, the following calculation for l_{max} is used

$$l_{max} = 0.1 \qquad \forall\, NC_{Tr} = 1 \tag{19}$$

$$l_{max} = \frac{\sqrt{A_{Tr}}}{4} \cdot \gamma \qquad \forall\, NC_{Tr} = 2 \tag{20}$$

The capacity of a feeder is dimensioned to supply the estimated demand of customers. The sizing of power lines depends on power demand, voltage quality, and minimum allowed tripping time. Tripping times refers to the minimum time before a protection device trips during a fault. Tripping times impact cable sizing as they impact the minimum needed fault impedance that is required to generate a sufficiently high fault current. Tripping times is regulated in national standards, Sweden [20], Germany [21] and the UK [22]. Cable size is iteratively evaluated until all conditions are fulfilled (see Fig. 4 for a flow chart of the process and Table 5 for cable parameters).

To calculate the feeder's required capacity, we assume a fixed three-phase fuse rating for each dwelling type. Even though single-phase connections are commonly used in the UK, the single-phase connection is made from the point of common connection to the household using a short service cable. The service cable is generally very short (tens of meters) and is excluded from the analysis.
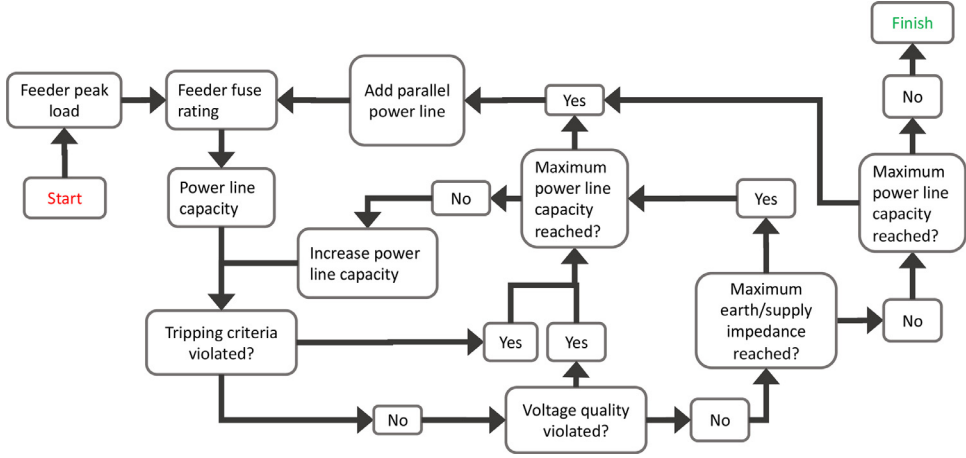
Fig. 4. Flow chart describing the process to size cables and power lines using criteria for thermal capacity, voltage limit, tripping times and maximum earth (Sweden) or supply (Germany and the UK) impedance.

Peak demand at position j of the feeder is then calculated as

$$I_{max,j} = \left(\text{Fuse}_{Apt} \cdot f(\rho) + \text{Fuse}_{House} \cdot (1 - f(\rho))\right) \cdot h\left(NC_{Apt,j} + NC_{House,j}\right) \tag{21}$$

where h is the coincidence factor as a function of number of customers and is obtained from Eqs. (6)-(12), $NC_{Apt,j}$ and $NC_{House,j}$ is the corresponding number of customers supplied from position j and U_{LL} is the line-to-line voltage. As each branch is equal, it is sufficient to calculate the aggregated voltage drop at each branch location and the voltage drop at the last position of the last branch. Power lines thermal limit is dependent on local environmental conditions. Feeder's thermal limit is therefore set based on PVC insulated underground cables at 20 °C [16]. If the highest capacity cable type cannot supply the number of connections while fulfilling tripping times and voltage quality limits, it is assumed that cables are used in parallel until all criteria can be fulfilled. Finally, we compare the earth fault impedance (Sweden [25]) and supply impedance (Germany and UK [26]) from our generated grids with reported and measured values and adjust cable sizes accordingly, see Eqs. (22)–(23).

$$Z_{max,earth} \geq Z_{cable,earth,j} + Z_{Tr,earth} \tag{22}$$

$$Z_{max,supply} \geq Z_{cable,j} + Z_{Tr} \tag{23}$$

Hosting capacity calculation

Hosting capacity is calculated by iteratively adding solar PV systems simultaneously at each customer location until operational limits area reached. The solar PV system are added in increments of 0.5 kW for each household until either the thermal or voltage quality limit is reached (step n). The solar PV systems are assumed to be three-phase and operate at unity power factor. Most solar PV installations today are three phase, with the exception of UK, where most customers are connected with a single-phase supply. However, the three-phase supply in the UK is often distributed into single-phase supply at the service cable level. We use a simplified voltage drop calculation [27]. Actual test feeders were used to compare an exact with a simplified voltage drop calculation and the error was found to be insignificant compared to other assumptions. Voltage at time t at the customer furthest away on the feeder is given by

$$U_{Cust,i}(t) = U_N - \frac{R_{Tr} \cdot NC_{Tr} \cdot \left(h(NC_{Tr}) \cdot P_{D,avg}(t) - PV_i(t)\right) - X_{Tr} \cdot NC_{Tr} \cdot h(NC_{Tr}) \cdot P_{D,avg}(t) \cdot pf}{U_N}$$

$$- \sum_{j=1}^{p} \frac{NC_{f,j} \cdot \left(R_{line,j} \cdot \left(h(NC_j) \cdot P_{D,avg,j}(t) - PV_i(t)\right) + \left(X_{line,j} \cdot h(NC_j) \cdot P_{D,avg,j}(t) \cdot pf\right)\right)}{U_N}$$

$$(24)$$

where $U_{Cust,i}$ is the voltage at the customer furthest away from the transformer, U_N is the nominal line-to-line voltage (400 V), $R_{line,j}$ and $X_{line,j}$ is the power line impedance for the low voltage feeder at branch j, R_{Tr} and X_{Tr} is the transformer impedance, p the number of branches per feeder, NC_j number of customers at point j, NC_{Tr} number of customers supplied by the transformer, and $h(NC)$ the coincidence function for NC number of customers and pf customers power factor. According to European regulations, voltage limit is calculated using 10 min variations from nominal voltage. We therefore use country specific 10 min annual load profiles based on customer type ($P_{D,Apt}(t)$ and $P_{D,House}(t)$). $P_{D,avg,j}$ is the average load profile based on the mix of house and apartment customers at position j in the feeder.

$$P_{D,avg,j}(t) = \frac{(NC_{Apt,j} \cdot P_{D,Apt,j}(t) + NC_{House,j} \cdot P_{D,House,j}(t))}{NC_{Apt,j} + NC_{House,j}} \tag{25}$$

The solar PV generation profiles (PV_i) for the solar PV installations are created using the modelling framework presented in [28]. The model is an empirical model based on [29,30] and assumes the solar PV systems are orientated in a southern direction, maximizing their peak power output. Meteorological input data for the solar PV modelling is from the MERRA-2 dataset for the year 2012 [31]. The dataset has a spatial resolution of 0.5° latitude and 0.625° longitude, and a temporal resolution of 1 h. The voltage limit is implemented as per unit values (p.u.), shown in Eq. (26). European regulations allow voltage variation of +/- 10% in the low-voltage grid, in agreement with National regulations in Sweden, Germany and the UK. National standards for distributed generation in Germany (VDE-AR-N 4105 [32]) states a maximum 3% voltage rise due to solar PV. A recent survey amongst German DSOs found that two out of ten surveyed DSOs, follows the 3% voltage rise standard. We use a previously suggested 5% voltage rise [33]. Since we exclude impacts in the medium-voltage grids, using a 5% voltage rise rather than 10%, we allow for a margin of voltage rise in the medium-voltage grid.

$$U_{(p.u)}^U pper \leq 1.05 p.u \tag{26}$$

The net power demand at each transformer is based on the total number of customers per transformer, their net demand and coincidence. The net power demand per transformer then becomes

$$P_{D,net}(t) = (h(NC_{TR}) \cdot P_{D,avg}(t) - PV(t)) \cdot NC_{TR} \tag{27}$$

The thermal limit for each transformer and cable is implemented as a hard limit, e.g. power transfer through the transformer cannot exceed its current carrying capacity at any given time. Shown in Eqs. (28) and (29).

$$\max\left(|P_{D,net}(t)|\right) \leq TR_{cap} \tag{28}$$

$$\max\left(|P_{D,net,j}(t)|\right) \leq Feeder_{Cap,j} \tag{29}$$

where $Feeder_{cap,j}$ is the feeder thermal capacity at location j. Hosting capacity expressed as individual household (HH) solar PV systems becomes:

$$PV_{HH} = PV_n \tag{30}$$

where PV_n is the PV capacity reached at the iteration before grid limitations are reached. As each transformer area is identical, the hosting capacity in kW per grid cell becomes:

$$PV_{Area} = PV_n \cdot NC \tag{31}$$

Table 6

Main model input and sources.

Input dataset	Load profiles (and annual electricity consumption for Sweden)	Low-voltage regulations	Dwelling distribution	Population density	Solar PV generation profiles
Sweden	[34]	[20]	[9]	[10]	[28]
Germany	[12]	[21]	[9]	[35]	[28]
UK	[36]	[22]	[9]	[35]	[28]

Table 7

General model parameters, values, and sources.

Parameter	α	γ_{City}	γ_{urban}	γ_{rural}	pf	$Fuse_{Apt}$	$Fuse_{House}$
Value	1.8	1.2	1.1	1	0.95	10A	20A
Source	[37]	[2]	[2]	[2]	Assumed	Assumed	Assumed

Table 8

Swedish specific model parameters, values, and sources for Household size and the Velander equation. Household size has been adjusted up for the results to be consistent with total number of households in Sweden.

Parameter	Household size$_{Apt}$	Household size$_{House}$	$k_{1,Apt}$	$k_{2,Apt}$	$k_{1,House}$	$k_{2,House}$
Value	2	2.7	0.000264	0.014	0.0003	0.0375
Source	[38]	[38]	[39]	[39]	[39]	[39]

Table 9

UK specific model parameters, values and sources for household size and ADMD coefficients.

Parameter	Household size	Ft	$ADMD_{Apt}$	$ADMD_{House}$
Value	2.35	0.7	1.5	2.1
Source	[40]	[11]	[11]	[11]

Table 10

German specific model parameters and parameter values for household size and coincidence for infinity number of customers.

Parameter	Household size	g_{∞}
Value	2	0.3
Source	[41]	[13]

Model data, parameters and sources

This section contains main data sources, parameter values and parameter sources for Sweden, UK and Germany. Table 6 shows sources for datasets for load profiles, regulations, dwelling distribution, population density and solar PV production profiles. Table 7 contains main model parameter values and sources. Tables 8-10 contains country specific parameter values and sources. Table 9

Method validation

The original research article [8] includes a validation of maximum feeder length and transformer density from the method as well as a comparison between model output and case studies. This section therefore focuses on the technical aspects of the model output. Fig. 5 shows model output of supply impedance for Sweden (A), Germany (B) and the UK (C). Supply impedance measure how strong the supplying grid is, where a lower supply impedance corresponds to a stronger grid. As our model exclude the supplying grid, supply impedance includes the low-voltage grid only. Even though high voltage levels also add impedance, the impact is often smaller than from the low-voltage grids. For Sweden the output is compared to the design impedance, and a reported maximum supply impedance
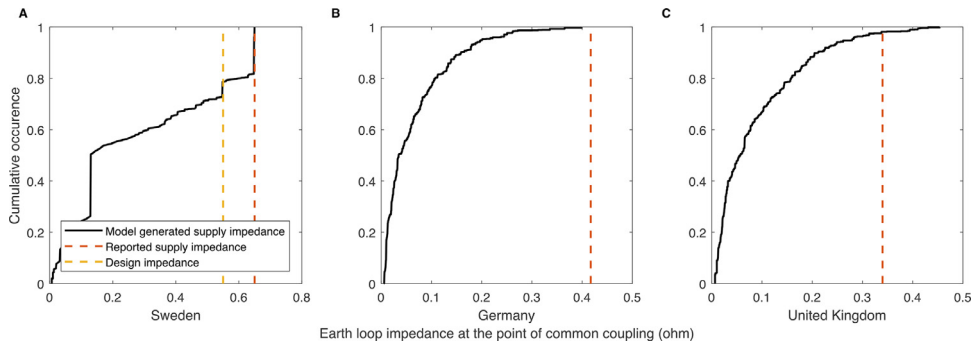
Fig. 5. Model output of supply impedance compared with reported and design values for Sweden (A), Germany (B) and UK (C).

for low-voltage customers [25]. For Germany and the UK, comparisons are done with the reported supply impedance from the IEC [26]. The comparison with IEC values for Germany and the UK is based on values from 1980, and was initially reported to cover 95% of the customers in Germany and 90% in the UK. As stated in the report, grid reinforcement activities have increased grid strength since, and the 90% limit is estimated to be 95% as of 2012.

As shown by Fig. 5, Sweden seems to have the highest supply impedance in the low-voltage grids, which would suggest a weaker low-voltage grid. However, it should be noted that Swedish low-voltage grids supply significantly fewer households, 11 households compared to 45 households in Germany and 67 households in the UK. Thus, on average, the supply impedance per customer is lower in Sweden, which has an impact on the grid's ability to support end-use technologies. The difference is explained by the larger share of rural population in Sweden compared to Germany and the UK. In Sweden, 2.7% of the population live in areas with a population density of 10 people/km^2. Comparing our results to Hernando-Gil et al. [42], whom estimated the supply impedance in the UK, we find that our estimates are lower than their corresponding low estimates. The difference is likely due to that Hernando-Gil et al. include the supply impedance from the medium voltage level as well as low-voltage level.

The requirement of 10 minutes annual load profiles in the method limited the choice of countries. Even though load profiles with hourly resolution are common in the literature, regulations on voltage variation are defined on a 10 min basis. Using load profiles with an hourly resolution would therefore underestimate voltage (and thermal) violations. In areas where voltage variations are a key determinant, the use of hourly load profiles would likely lead to a larger estimate of grid capacity. Annual load profiles with a 10 min resolution are rare. The input datasets therefore only contained few load profiles, which might not include variation that is commonly found amongst households. Access to larger datasets could reduce this error, but also increase computation time.

The model relies on the estimation dwelling type (Fig. 2) to calculate power demand in each grid cell. As seen in Fig. 2, there are significantly fewer datapoints for Sweden than Germany or the UK, which is also reflected in the corresponding R^2 values. The extrapolation likely causes more issues in grid cells where a significant share of the area contains non-residential uses, such as industrial areas or parks and recreation areas. If higher resolution data would be available, the estimated share of single-family houses could be improved, leading to a better estimated power demand. This could potentially be achieved using satellite data to identify number of single-family houses in the respective grid cells.

Declaration of Competing Interests

The authors declare that they have no known competing financial interests or personal relationships that could have appeared to influence the work reported in this paper.

The authors declare the following financial interests/personal relationships which may be considered as potential competing interests:

References

[1] E. Hartvigsson, M. Odenberger, P. Chen, E. Nyholm, Dataset for generating synthetic residential low-voltage grids in Sweden, Germany and the UK, Data Brief 36 (2021) 107005.
[2] M. Hyvärinen, "Electrical networks and economies of load density," Helsinki University of Technology, 2008.
[3] T. Jamasb, M. Pollitt, Reference models and incentive regulation of electricity distribution networks: an evaluation of Sweden's network performance assessment model (NPAM), Energy Policy 36 (5) (2008) 1788–1801.
[4] C.M. Domingo, T.G.S. Roman, Á. Sanchez-Miralles, J.P.P. Gonzalez, A.C. Martinez, A reference network model for large-scale distribution planning with automatic street map generation, IEEE Trans. Power Syst. 26 (1) (2011) 190–197.
[5] D. Pudjianto, P. Djapic, J. Dragovic, and G. Strbac, "Grid Integration Cost of PhotoVoltaic Power Generation," London, 2013.
[6] J. Widén, E. Wäckelgård, J. Paatero, P. Lund, Impacts of distributed photovoltaics on network voltages: stochastic simulations of three Swedish low-voltage distribution grids, Electric Power Syst. Res. 80 (12) (2010) 1562–1571.
[7] E. Nyholm, M. Odenberger, F. Johnsson, An economic assessment of distributed solar PV generation in Sweden from a consumer perspective – the impact of demand response, Renew. Energy 108 (2017) 169–178.
[8] E. Hartvigsson, M. Odenberger, C. Peiyuan, E. Nyholm, Estimating grid capacity for residential solar photovoltaic in Sweden, UK and Germany, Renew. Energy (2021).
[9] Eurostat, "2011 Census," 2011.
[10] Statistics Sweden, Population density, Geodata Stat. (2018).
[11] C. Barteczko-Hibbert, Report, 2015.
[12] VDI, VDI 4655: Reference load profiles of single-family and multi-family houses for the use of CHP systems, Düsseldorf (2008).
[13] H. Ruf, Limitations for the feed-in power of residential photovoltaic systems in Germany – An overview of the regulatory framework, Sol. Energy 159 (Jan. 2018) 588–600.
[14] T. Haggis, "Network Design Manual," Coventry, 2006.
[15] Energimarknadsinspektionen, "Normvärdeslista," Stockholm, 2015.
[16] Svenska Elektriska Kommissionen, Vagledning for dimensionering av ledningsnat for lagspanning, SEK, 4th ed., 2005.
[17] U.S Energy Information Administration, "Power outages often spur questions around burying power lines," 2012. .
[18] SCB, "Statistics Sweden, Open Geodata," 2019. .
[19] Lantmateriet, "GSD-Terrängkartan, vektor,", Gavle (2019).
[20] Svenska Elektriska Kommissionen, "SS 424 14 06 (Methods of calculation to safeguard correct disconnection – Single cable in a directly earthed system protected by fuses (simplified method))," 2005.
[21] VDE, "DIN VDE 0100-410," Berlin, Germany, 2018.
[22] IET, "Requirements for Electrical Installations - BS7671." IET, Stevenage, 2018.
[23] Svensk ElstandardVagledning for dimensionering av ledningsnat for lagspanning, Svensk Elektriska Kommisionen, 2016.
[24] NKTN1XV 0,6/1 kV specification, NKT, 2021.
[25] P. Norberg, A. Larsson, M. Sundell, and U. Grape, "Introducing network strength to handle power qualityin system planning," Paris, France, 2008.
[26] IEC, *IEC 60725:2012*. Geneva: International Electrotechnical Comission, 2012.
[27] P. Chen, T. Thiringer, Time-series based cable selection for a medium voltage wind energy network, IEEE Trans. Sustainable Energy 3 (3) (2012) 465–473.
[28] Z. Norwood, E. Nyholm, T. Otanicar, F. Johnsson, A geospatial comparison of distributed solar heat and power in Europe and the US, PLoS One 9 (12) (2014) e112442.
[29] D. L. King, W. E. Boyson, and J. A. Kratochvill, "Photovoltaic Array Performance Model," Livermore, Calofornia, 2004.
[30] T. Huld, et al., A power-rating model for crystalline silicon PV modules, Sol. Energy Mater. Sol. Cells 95 (12) (2011) 3359–3369.
[31] Global Modeling and Assimilation Office GMAO), "MERRA-2 tavg1_2d_rad_Nx: 2d,1-Hourly, Time-Averaged,Single-Level,Assimilation,Radiation Diagnostics V5.12.4. 2015," Greenbelt, MD, USA, 2012.
[32] DIN-VDE, *VDE-AR-N 4105: Power Generation Systems Connected to the Low-voltage Distribution Network*. 2011.
[33] M.H.J. Bollen, P. Verde, A Framework for regulation of RMS voltage and short-duration under and overvoltages, IEEE Trans. Power Delivery 23 (4) (2008) 2105–2112.
[34] J.P. Zimmerman, End-use metering campaign in 400 households In Sweden assessment of the potential electricity savings, Eskilstuna (2009).
[35] Eurostat, "GEOSTAT Population grid," Luxembourg, 2011.
[36] D. Murray, L. Stankovic, V. Stankovic, An electrical load measurements dataset of United Kingdom households from a two-year longitudinal study, Sci. Data 4 (Jan. 2017) 160122.
[37] UK Power and Networks, "Design and Planning: Framework for underground networks in UK Power Networks," 2011.
[38] Statistics Sweden, "Antal personer per hushåll efter region och boendeform," 2018. .
[39] I. U. D. Igor Satori, Joana Ortiz, Jaune Salom, "Estimation of load and generation peaks in residential neighbourhoods with BIPV: bottom-up simulations vs. Velander," in *World Sustainable Building*, 2014.
[40] Office for National Statistics, "Families and households in the UK: 2019," Newport, 2019.
[41] Eurostat, "Household composition statistics," Luxembourg, 2019.
[42] I. Hernando-Gil, H. Shi, F. Li, S. Djokic, M. Lehtonen, Evaluation of fault levels and power supply network impedances in 230/400 V 50 Hz generic distribution systems, IEEE Trans. Power Delivery 32 (2) (2017) 768–777.
[43] Electrical Engineering Toolbox, "Resistance and Reactance per km of Copper and Aluminium cables."2021.